Available online at www.sciencedirect.com
SCIENCE DIRECT®
Journal of Electron Spectroscopy and Related Phenomena 136 (2004) 143–150
JOURNAL OF ELECTRON SPECTROSCOPY and Related Phenomena
www.elsevier.com/locate/elspec

Polarization dependence in resonant soft X-ray emission spectroscopy of 3*d* transition metal compounds

Yoshihisa Harada [a], Shik Shin [a,b,*]

[a] *RIKEN/Spring-8, 1-1-1 Kouto, Mikazuki-cho, Sayo-gun, Hyogo 679-5148, Japan*
[b] *The Institute for Solid State Physics, University of Tokyo, Kashiwanoha 5-1-5, Kashiwa, Chiba 277-8581, Japan*

Abstract

We report experimental studies of polarization dependence in resonant soft X-ray emission of 3*d* transition metal compounds. In metal 2*p* resonant soft X-ray emission spectra of $3d^0$ systems, transition to the bonding and antibonding states between $3d^0$ and $3d^1\underline{L}$ configurations shows polarization dependence. In TiO_2, the polarization dependence is drastic, whereas it is slightly weak in ScF_3 and extremely weak in $KMnO_4$. The results are explained by a local symmetry selection rule, strength of hybridization, and phase relation of wave-functions among initial, intermediate, and final states. In oxygen 1*s* resonant excitation of undoped cuprate, $Sr_2CuO_2Cl_2$, we demonstrate that Zhang–Rice singlet excitation, *dd* excitation, as well as two spin-flip excitations can be distinguished according to their symmetry.

PACS: 78.70.En; 71.35.Gg; 74.72.-h

Keywords: Soft X-ray emission; Polarization dependence; Symmetry

1. Introduction

In the last decade we have experienced rapid progress in the soft X-ray spectroscopy. Using brilliant synchrotron radiation as an excitation source, we obtain a specific core excited state by tuning excitation energy and polarization. The most benefited one from this is the resonant soft X-ray emission spectroscopy (RSXES) [1,2]. In RSXES core excitation and decay process occurs coherently. Energy difference between incident and emitted photons corresponds to the energy of an elementary excitation left in the final state. Recently a number of RSXES spectra are reported on semiconductors [3–7], transition metal compounds [8–16], and rare earth compounds [17], with the development of technologies in gratings and detectors that improves the energy resolution of a soft X-ray emission spectrometer up to 1000 ($E/\Delta E$). For lots of RSXES spectra, elementary excitations have been identified by excitation energy dependence and detailed comparison with other spectroscopic results, such as X-ray absorption spectroscopy (XAS) and photoemission spectroscopy (PES). In the meantime, we can obtain information about symmetry of elementary excitations by measuring polarization dependence in RSXES [18]. There exists, however, very few previous works on solids where practical measurements and corresponding analysis are made on polarization dependence in RSXES [19]. The RSXES process is described by the Kramers Heisenberg formula

$$F(\Omega,\omega)=\sum_{T_2}\sum_{j}\left|\sum_{i}\frac{\langle j|T_2|i\rangle\langle i|T_1|g\rangle}{E_g+\Omega-E_i-i\Gamma}\right|^2 \times\delta(E_g+\Omega-E_j-\omega), \quad (1)$$

where Ω and ω are the incident and emitted photon energies, $|g\rangle$, $|i\rangle$, and $|j\rangle$ are initial, intermediate, and final states of the material system, respectively, E_g, E_i, and E_j are their energies, and Γ represents the spectral broadening due to the core-hole lifetime in the intermediate state. The dipole transition operator T_1 and T_2 are taken in the direction of incident and emitted photon polarization. We obtain symmetry of the final state dependent on the incident and emitted photon polarization. In this paper, we review our recent RSXES studies on 3*d* transition metal compounds which well describe the advantage of polarization dependence.

* Corresponding author. Tel.: +81-471-36-3381; fax: +81-471-36-3383
E-mail address: shin@issp.u-tokyo.ac.jp (S. Shin).

0368-2048/$ – see front matter © 2004 Elsevier B.V. All rights reserved.
doi:10.1016/j.elspec.2004.02.141

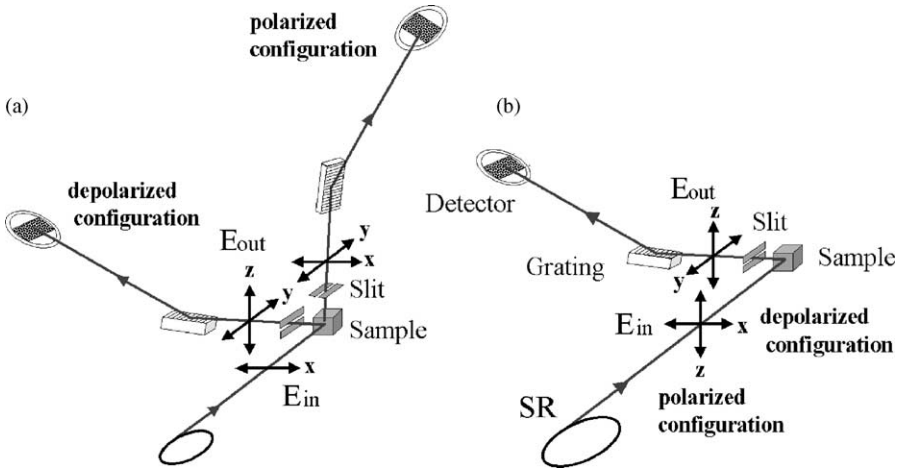

Fig. 1. Schematic drawing of the experimental configuration. (a) Normal planar undulator; (b) figure-8 undulator.

2. Experimental details

We studied polarization dependence in RSXES with metal $2p$ edge excitation of TiO_2, ScF_3, $KMnO_4$ and with oxygen $1s$ edge excitation of $Sr_2CuO_2Cl_2$. The samples are a rutile single crystal of $TiO_2(0\,0\,1)$, pressed pellets of ScF_3 powder and $KMnO_4$ powder, and a single crystal of $Sr_2CuO_2Cl_2$ grown by the melt. We have installed soft X-ray emission spectrometers with polarization dependence at beamline (BL) 2C in Photon Factory (PF) and at BL27SU in SPring8. (Figure 1 shows schematic drawing of two experimental configurations to study polarization correlation in

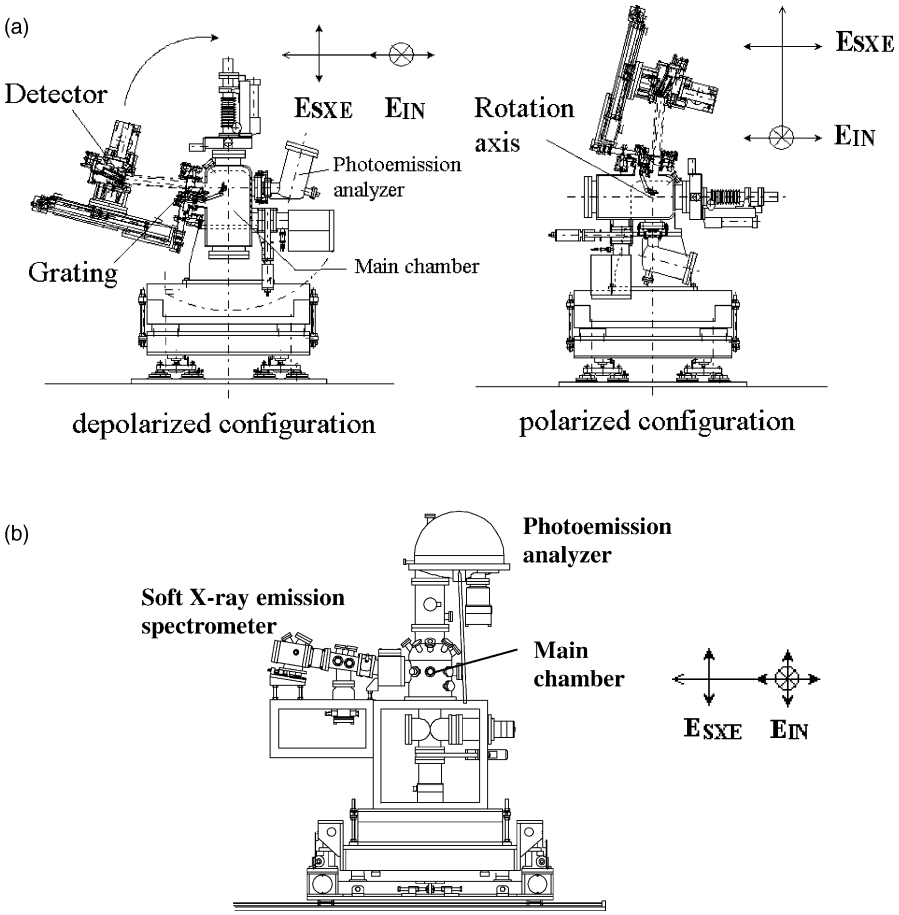

Fig. 2. Front view of the soft X-ray emission spectrometer system at (a) BL2C in Photon Factory and (b) BL27SU in SPring8. The axis of the incident beam is perpendicular to the drawing. Arrows with E_{IN} and E_{SXE} labels indicate polarization vector of incident photon and soft X-ray emission, respectively.

RSXES. The wave vectors of incident and emitted photons form a scattering plane, and the scattering angle is fixed to 90°. When the polarization vector of the incident photon is parallel to the scattering plane, it is called "depolarized configuration" while when the polarization vector of the incident photon is perpendicular to the scattering plane, it is called "polarized configuration". It is noted that both the polarization-contained and the polarization-rotated components equally contribute to emission spectra in the polarized configuration, while only the polarization-rotated one is included in the depolarized configuration. In terms of the Raman tensor, a polarization-contained component corresponds to diagonal elements, and a polarization-rotated component corresponds to off-diagonal elements. It is favorable to perform complete analysis of polarization correlation between incident and emitted photons, however, it is difficult to separate soft X-ray emissions by their polarizations because a soft X-ray polarimeter is still in a developmental stage, and is not yet available commercially. As shown in Fig. 1(a), we have conducted a rotation of an experimental chamber around the axis of the incident beam at BL2C in PF due to a normal planar undulator that provides linearly polarized incident photon fixed in the horizontal plane (Fig. 2(a)) shows a front view of the system [20]. An analyzer chamber equipped with the emission spectrometer rotates 90°around the axis of the incident beam. The analyzer chamber is sealed with two differentially pumped rotary feed-throughs, and separated from the beam line using a vacuum valve. The emission spectrometer is based on the Rowland circle geometry with the best energy resolution of more than 1000 ($E/\Delta E$) using three holographic spherical gratings that cover the energy range from 18 to 1200 eV, and served as the first soft X-ray emission spectrometer with polarization dependence in Japan. The energy resolution for the incident and the emitted photons applied in this study is summarized in Table 1.

We made the alternative experimental configuration by using a light source which is able to switch linear polarization from vertical to horizontal, as shown in Fig. 1(b). This is exactly the same in geometry as the rotation of the experimental chamber. Our system in SPring8 employed the figure-8 undulator alternatively as a light source, where the incident beam has both vertical and horizontal polarization [21]. As shown in Fig. 2(b), the emission spectrometer is rigidly mounted on the base plate of the experimental chamber. This has greatly improved the stability of the measurement system. The emission spectrometer is based on the flat field focusing geometry with two varied line-spacing holographic spherical gratings that cover the energy range from 250 to 900 eV [22]. The emission spectrometer was dedicated to balance high energy resolution around 1000 ($E/\Delta E$) with high detection efficiency. By using this experimental, we will measure polarization dependence of the materials very precisely.

Table 1
Energy resolution for the incident and emitted photons

Sample	Subshell	ΔE_{in}(eV)	ΔE_{out}(eV)
ScF_3	Sc 2p	0.2	0.6
TiO_2	Ti 2p	0.1	0.4
$KMnO_4$	Mn 2p	0.4	1.2

3. Results and discussion

3.1. Ti2p RSXES on TiO_2 [23]

First we discuss Ti 2p absorption and emission results on TiO_2. TiO_2 is a representative of a $3d^0$ system, and the character of the electronic states near the energy gap has long been discussed in terms of both delocalized and localized description. Figure 3 shows (a) Ti 2p XAS and (b) Ti 2p RSXES with polarization dependence. The XAS spectrum was obtained by the total electron yield method. The excitation energies for RSXES are indicated on the XAS spectrum. RSXES spectra are plotted relative to the energy-loss from

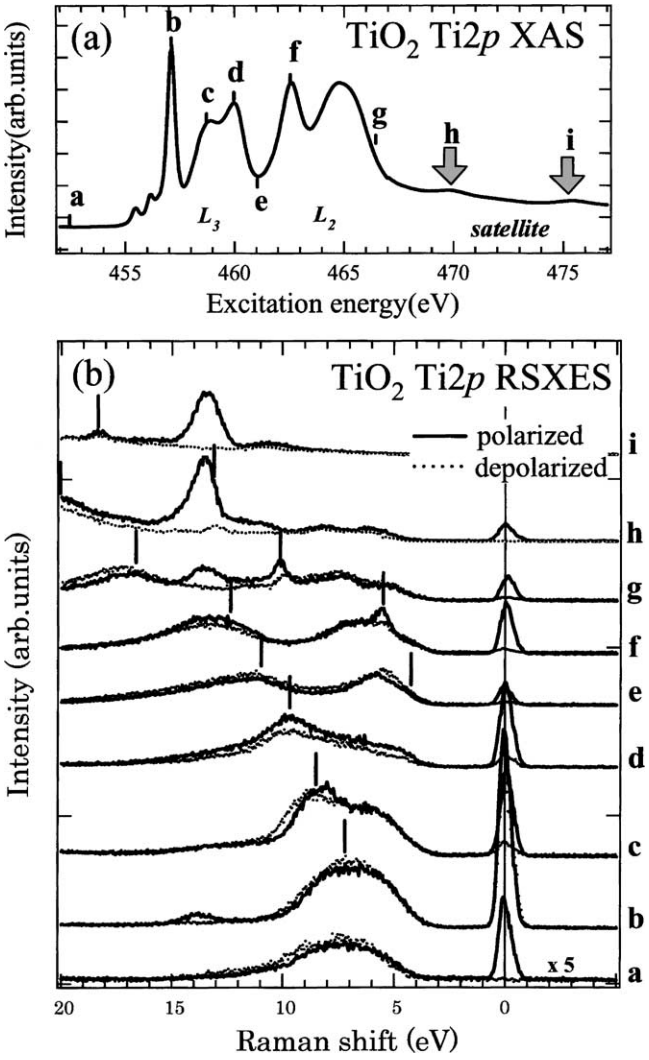

Fig. 3. (a) Ti 2p XAS spectrum and (b) Ti 2p RSXES spectra of TiO_2. Solid bars on each RSXES spectrum indicate peak positions of the fluorescence.

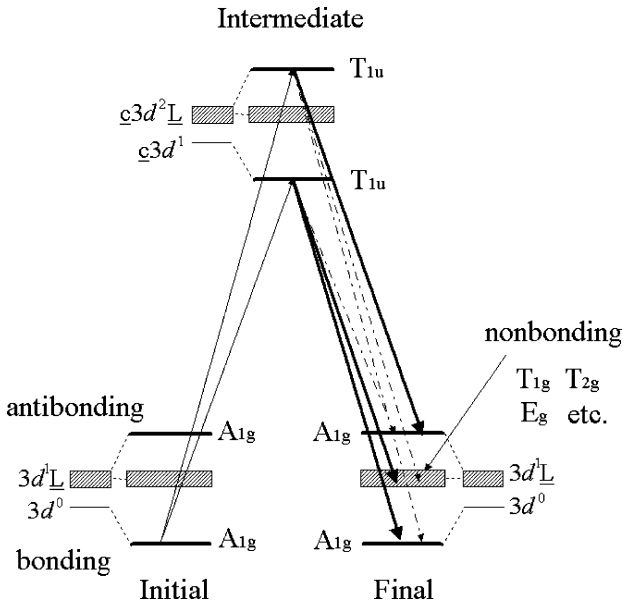

Fig. 4. Schematic energy level diagram for RSXES of TiO_2.

the recombination peaks (we show below all the spectra of the $3d^0$ systems in the same form). Two types of emissions are present in this plot, one staying almost at the same energy and the other shifting with the excitation energy. The former is a soft X-ray Raman scattering that accompanies valence excitations. When the excitation energy is set to the satellite region in the XAS spectrum, dramatic enhancement occurs only in the former structure in the polarized configuration: giant enhancement of 14 eV energy-loss structure in the spectra labeled h and i. Small enhancement is also observed in the spectrum labeled b. This structure has an energy loss which is too large to be associated with the valence band structure, so that it is difficult to be analyzed using a band calculation. In fact, it is related to a localized electronic structure, and we can give an interpretation for this based on a cluster model combined with configuration interaction approximation. The energy level diagram for RSXES of TiO_2 is shown schematically in Fig. 4. TiO_2 is nominally in the $3d^0$ state, but actually the $3d^0$ configuration is strongly mixed with a charge transferred $3d^1\underline{L}$ configuration by the covalency hybridization. The ground state is the bonding state between the $3d^0$ and $3d^1\underline{L}$ configurations, and the antibonding state is located about 14 eV above the ground state with the cluster model parameters used by Okada and Kotani [24]. If we assume, for simplicity, the O_h symmetry for the cluster as done by Okada and Kotani, both bonding and antibonding states are specified by an irreducible representation A_{1g}. In addition to these states, there are nonbonding $3d^1\underline{L}$ states with A_{2g}, T_{1g}, T_{2g}, E_g . . . irreducible representations located near the middle of the bonding and antibonding energy levels. When a Ti $2p$ electron is excited to the $3d$ state by an incident photon, we have $\underline{c}3d^1$ and $\underline{c}3d^2\underline{L}$ configurations which are mixed strongly by the covalency hybridization. The main peak of the Ti $2p$ XAS corresponds to the bonding state between the $\underline{c}3d^1$ and $\underline{c}3d^2\underline{L}$ configurations, while the satellite corresponds to the antibonding state between them. The intensity of the satellite is very weak because of the phase cancellation between the wave functions of the ground and photo-excited states. Also, the X-ray absorption is almost forbidden to the nonbonding $\underline{c}3d^2\underline{L}$ states. In Fig. 4, for simplicity, we disregard the effects of the spin–orbit splitting of the $2p$ states and the crystal field splitting of the $3d$ states. The resonantly excited intermediate states, which correspond to the main peak and the satellite of the XAS, decay radiatively to each of the final states, i.e. the bonding, nonbonding and antibonding states. It is shown from Eq. (1) and group theoretical consideration that the final states with A_{1g}, T_{1g}, T_{2g}, and E_g irreducible representations are allowed in the polarized configuration, whereas those with only T_{1g} and T_{2g} irreducible representations are allowed in the depolarized configuration. Therefore, the recombination peak (bonding state) and the 14 eV inelastic peak (antibonding state) are allowed in the polarized configuration, but they are forbidden in the depolarized configuration. The nonbonding states are allowed both in the polarized and depolarized configurations. They are observed in Fig. 3 as broad structures from 3 to 10 eV with weak polarization dependence below the recombination peak. In Fig. 3, the structure shifting with the excitation energy (indicated by vertical bars in Fig. 3(b)) has almost the same energy when plotted against the emission energy. This corresponds to a so called momentum-conserved Raman scattering observed in various semiconductors [3–7], which converges to the fluorescence at higher excitation energies. Idé and Kotani [25] has reproduced the structure by a multi-site cluster model which accounts for translational symmetry in the localized model. In the above analysis, polarization dependence plays a decisive role to settle the controversy over the origin of the satellite structures observed in the Ti $2p$ XAS of TiO_2 [24]. Moreover, the RSXES shows that TiO_2 has both delocalized [26–32] and localized [33–38] electronic structures, the latter showing remarkable polarization dependence only explained by the cluster model with configuration interaction. It is noted that resonant enhancement of RSXES to different final states with same symmetry, like bonding and antibonding states, occurs at different excitation energies. As explained above for the absorption process, it is due to phase relation between wave-functions of core-excited and final states. If the core-excited state has bonding/antibonding character, the bonding/antibonding state in the final state is 'in phase' and has large cross section in the emission process. We show some other results on $3d^0$ systems where characteristics of the electronic structure is reflected on the polarization dependence in RSXES.

3.2. Sc $2p$ RSXES on ScF_3

Figure 5 shows (a) Sc $2p$ XAS and (b) Sc $2p$ RSXES of ScF_3. ScF_3 is also a $3d^0$ system with the O_h symmetry. RSXES spectra show polarization dependence around 15 eV

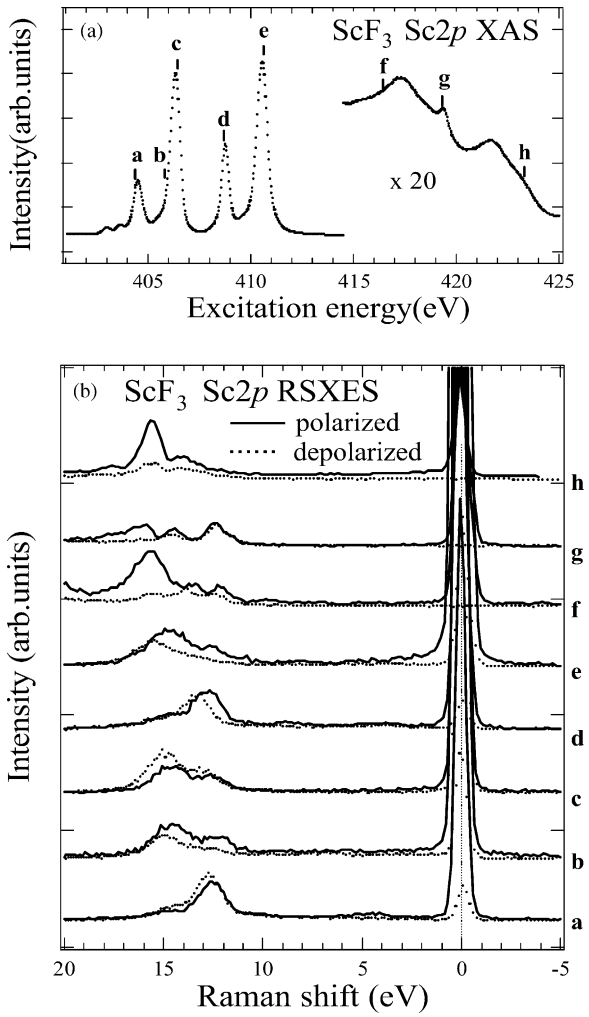

Fig. 5. (a) Sc 2*p* XAS spectrum and (b) Sc 2*p* RSXES spectra of ScF_3.

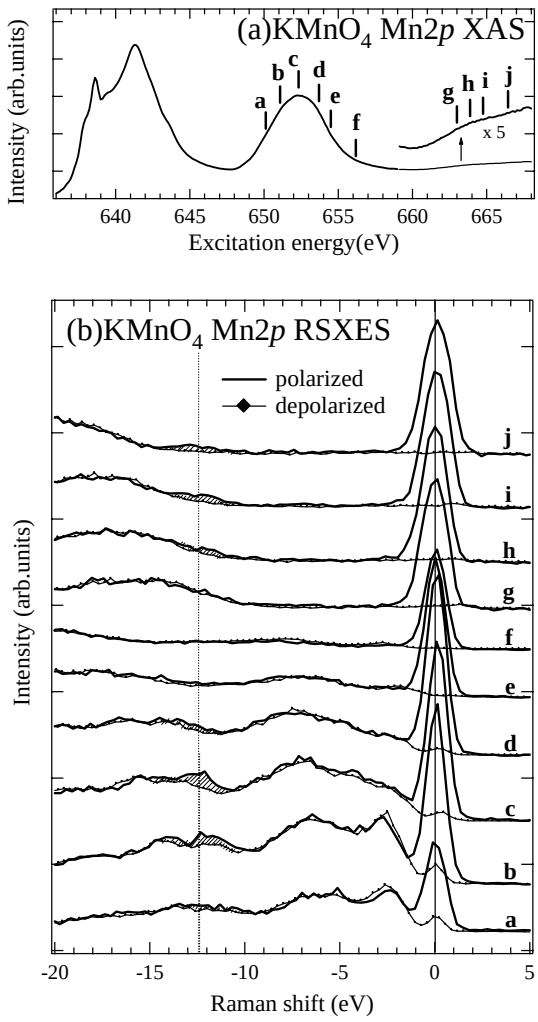

Fig. 6. (a) Mn2*p* XAS spectrum and (b) Mn2*p* RSXES spectra of $KMnO_4$. A small hump structure around 12 eV is indicated by hatched lines.

when measured with excitation to the antibonding state, although the enhancement in the polarized configuration is less drastic than that of TiO_2. Following the assignments for TiO_2, the structure around 15 eV can be ascribed to transition to the antibonding state between the $3d^0$ and $3d^1\underline{L}$ configurations. The antibonding state has structures, though the origin is not clear at present. The nonbonding state is located around 13 eV, which is much larger than that of TiO_2. This is because ScF_3 has similar value for the hybridization energy to TiO_2, but about three times larger (9 eV) charge transfer energy than TiO_2 [39]. Thus, the ratio of the effective hybridization energy to the charge transfer energy, a measure for the hybridization effect, is smaller than that of TiO_2. This may account for the less polarization dependence in ScF_3 [39]. This also leads to small occupancy of 3*d* electrons, which may account for the weak intensity of the fluorescence in ScF_3.

3.3. Mn2*p* RSXES on $KMnO_4$

For another example of a $3d^0$ system we show in Fig. 6(a) Mn 2*p* XAS and (b) Mn 2*p* RSXES of $KMnO_4$. $KMnO_4$ is nonmagnetic unlike other manganese oxides due to $3d^0$ character with its highest formal valency VII in the ground state. The local symmetry is nearly T_d, where the A_1 irreducible representation in the ground state has the same polarization dependence as A_{1g} irreducible representation in the O_h symmetry. As shown in Fig. 6, excitation energies are tuned around the onset of the satellite structures in the XAS. For $KMnO_4$, the Mn 2*p* spin–orbit splitting is comparable with the energy splitting of the bonding and antibonding states between the $3d^0$ and $3d^1\underline{L}$ configurations, so that L_3 satellite structures are severely overlapped with L_2 main structures in the XAS. In the RSXES spectra, around 12 eV below the recombination peak a small hump is found only in the polarized configuration, overlapped with L_3 and L_2 fluorescences. We can relate the hump structure to the antibonding state between the $3d^0$ and $3d^1\underline{L}$ configurations following the assignments for TiO_2 and ScF_3. It is consistent with the argument by Butorin et al. [8], where the presence of the same structure in RSXES around 13 eV below the recombination peak was suggested. Considering that $KMnO_4$

is highly covalent in a tetrahedral MnO_4^- cluster with a small charge transfer energy between the Mn 3d and O 2*p* states, one might expect strong enhancement of the antibonding state in the polarized configuration, referring to the comparison between TiO_2 and ScF_3. However, the experimental result shows opposite behavior: the enhancement of this structure in the polarized configuration is strongly suppressed compared with the case of TiO_2. This is also true for the satellite structures in the absorption spectrum. As pointed out by Reinert et al. [40], $KMnO_4$ shows a strong deviation from a purely ionic charge distribution: considerable occupation of Mn 3*d* electrons in the ground state. Thus, we expect high contribution from multiple charge transfer states $3d^n\underline{L}^n$ ($1 \leq n \leq 5$ or higher), which is possibly responsible for breaking of phase matching between core excited and ground states. We can explain an enhancement of the recombination peak at the satellite excitation in the same fashion. Note that, within dipole approximation, the recombination peak is always forbidden in the depolarized configuration in a $3d^0$ system. To further discuss the origin of the suppression, systematic data collection on $3d^0$ systems as well as close comparison with a theoretical calculation is necessary.

3.4. O 1*s* RSXES on $Sr_2CuO_2Cl_2$ [41]

Cuprate is another interesting target for RSXES because it has various low energy excitations deeply related to its electronic and magnetic properties. In particular, high Tc superconductors have been a focus of attention. Characteristics of high Tc superconductors are often described by the *t*–*J* model [42], where charge carriers are so-called Zhang–Rice singlet (ZRS) states [43]. It is well accepted that the ZRS is a coupled state of a Cu 3*d* hole and an O 2*p* state on a CuO_4 plaquette and moves around on the Cu–O network, breaking the antiferromagnetic order of Cu 3*d* localized-spins. Hence, it is quite important to investigate the characteristics of the ZRS. We show here a novel experimental method for the direct observation of the ZRS state in $Sr_2CuO_2Cl_2$ using polarization dependence in O 1*s* RSXES. In RSXES a Cu 3*d* hole is transferred to the neighboring Cu site mediated by an O 1*s* core hole in the intermediate state to leave the ZRS in the final state. So the ZRS formation in RSXRS accompanies an extra electron mainly in the Cu 3*d* states, in contrast to the ZRS formation in PES. $Sr_2CuO_2Cl_2$ is suitable for exploring oxygen states only in the Cu–O plane due to the absence of apical oxygen atoms. It is highly stoichiometric and cannot be readily doped, which ensures we are measuring a pure $Sr_2CuO_2Cl_2$ insulator. O 1*s* absorption and polarization dependence in O 1*s* RSXES of $Sr_2CuO_2Cl_2$ are displayed in Fig. 7. The main broad structure between 3 and 10 eV (denoted by main band) is the contribution from the O 2*p* valence band. The main band is a superposition of the Raman component following the excitation energy (mainly below the absorption edge) and a fluorescence-like component (mainly above the absorption edge). At the high energy side of the main band small structures exist that follow the excitation energy. It is remarkable that clear polarization dependence is found both in the recombination peak and the energy-loss structure around 2 eV, as well as the O 2*p* main band. First we discuss the structure around 2 eV. It is clearly seen that the intensity of the 2 eV structure is stronger in the polarized configuration than in the depolarized configuration. Kuiper et al. [19] determined the absolute Cu *dd* excitation energies of $Sr_2CuO_2Cl_2$ by RSXES spectra across the Cu 3*p* edge. The single hole at copper site in the ground state is ascribed to $d(x^2 - y^2)$ and from their analysis, $d(3z^2 - r^2)$, $d(xy)$ and $d(xz)$ ($d(yz)$) states are positioned at 1.5, 1.35, and 1.7 eV above the ground state, respectively. According to Abbamonte et al. [44], on the other hand, resonant X-ray Raman scattering spectra across the Cu 1*s* edge of $Sr_2CuO_2Cl_2$ exhibits a small and broad peak around 2 eV. Hill et al. [45] and Idé and Kotani [46] showed that the lowest energy inelastic peak of resonant X-ray Raman scattering across the Cu 1*s* edge of Nd_2CuO_4 corresponds to the ZRS excitation. Therefore, the possible origin of the 2 eV structure in Fig. 7 might be the ZRS excitation or the *dd* excitation (or the two excitations overlap each other). Okada and

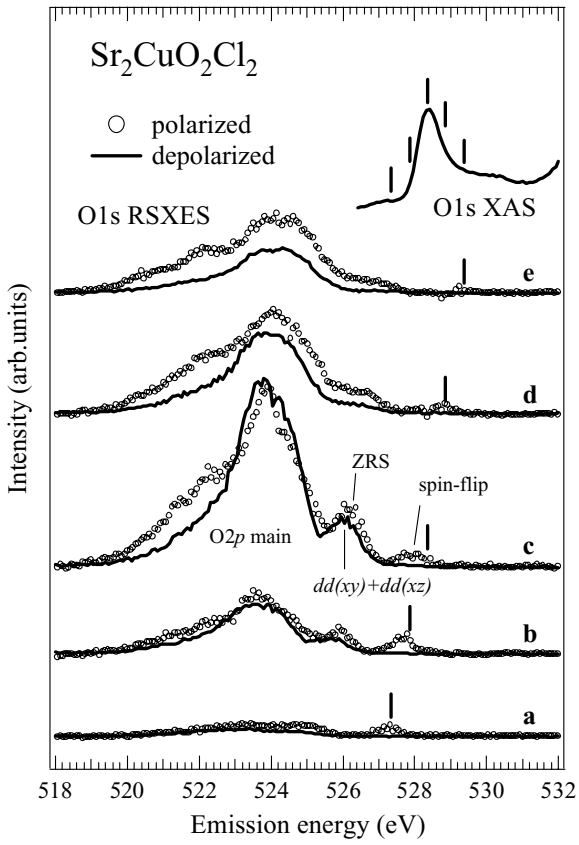

Fig. 7. Resonant soft X-ray emission spectra of $Sr_2CuO_2Cl_2$ across the O 1*s* excitation in the Raman shift representation. The open circles and the solid lines are the results for the polarized and depolarized configuration, respectively. O 1*s* RSXES shows a series of the emission spectra across the O 1*s* resonant excitation. O 1*s* XAS shows a soft X-ray absorption spectrum across the O 1*s* edge. Vertical bars on O 1*s* XAS and O 1*s* RSXES show the position of the incident photon energy.

Kotani predicted that the ZRS and the *dd* excitations have a comparable intensity in RSXES at the O 1*s* edge, whereas the former is dominant at the Cu 3*p* edge and the latter is dominant at the Cu 1*s* edge. An important point that Okada and Kotani predicted is that the ZRS and the *dd* excitations in RSXES at O 1*s* edge can be discriminated by selection rules of the polarization-dependence. As Okada and Kotani showed, the ZRS excitation in the O 1*s* RSXES is allowed only for the polarized configuration. Also, from a simple consideration of symmetry, the *dd* excitation of the $d(xy)$ state, which we call as $dd(xy)$ excitation hereafter, is allowed for the depolarized configuration, while the $dd(3z^2 - r^2)$ excitation is allowed for the polarized one. The $dd(xz)$ excitation is allowed for both configurations. According to a recent cluster-model calculation [47], which well reproduces the profile of the O 1*s* RSXES main band structure in this work including polarization dependence, the intensity of the $dd(3z^2 - r^2)$ and $dd(xy)$ excitation is nearly the same. In other words, without ZRS contribution, the intensity of the 2 eV structure does not depend on the experimental geometry. Therefore, we conclude that the enhanced 2 eV structure in the polarized configuration is caused by the ZRS contribution. In the spectra obtained by excitation 1 eV below the absorption peak (spectrum (a) in Fig. 7), the recombination peak with very weak shoulders exhibits polarization dependence. At peak excitation (spectrum (c) in Fig. 7), however, the elastic peak vanishes and only the energy-loss structures around 0.5 eV grow up to show clear polarization dependence. These structures have been confirmed not to originate from an elastic component due to a wrong energy calibration. It is found from Fig. 7 that the 0.5 eV peak is allowed only for the polarized configuration. Considering the polarization dependence and its energy position, we interpret it as the two-magnon excitation [48]. It is to be emphasized that the observation of the 0.5 eV peak is impossible in the Cu 3*p* RSXES because of the existence of the strong recombination peak, but it becomes possible in the present study by taking advantage of extremely weak elastic scattering intensity in the O 1*s* edge.

4. Conclusion

In conclusion, we have given a review of our recent experimental results on polarization dependence in RSXES of 3*d* transition metal compounds. In Ti 2*p* RSXES of TiO_2 and Sc 2*p* RSXES of ScF_3, polarization dependence is found when the excitation energy is tuned to the satellite structures in the absorption spectrum. The enhanced peak is ascribed to the antibonding state between the $3d^0$ and $3d^1\underline{L}$ configurations, which appears only in the polarized configuration due to the symmetry selection rule in RSXES. When the wavefunctions involved in the transition are "in phase", clear polarization dependence is found, whereas only a slight change in the inelastic peak is found in Mn 2*p* RSXES of $KMnO_4$, possibly due to breaking of phase matching between core excited and ground states by the participation of multiple charge transfer states. We have found that even ligand O 1*s* RSXES of $Sr_2CuO_2Cl_2$ show polarization dependence, which enables us to discriminate Zhang–Rice singlet excitation, *dd* excitation, as well as two spin-flip excitations. Not limited to 3*d* transition metal compounds, it is necessary to promote the use of polarization dependence in RSXES in terms of its exclusive role to provide information about symmetry of low energy excitations closely related to solid state properties.

Acknowledgements

We are very grateful to K. Okada, A. Kotani, and M. Matsubara for fruitful discussions. We acknowledge excellent support from the staff of Photon Factory and Y. Tamenori and H. Ohashi in SPring8. This work is supported by a Grant-in-Aid for Scientific Research from the Ministry of Education, Culture, Sports, Science and Technology in Japan.

References

[1] A. Kotani, S. Shin, Rev. Mod. Phys. 73 (2001) 203.
[2] F. Gel'mukhanov, H. Ågren, Phys. Rep. 312 (1999) 87.
[3] S. Shin, A. Agui, M. Watanabe, M. Fujisawa, Y. Tezuka, T. Ishii, Phys. Rev. B 53 (1996) 15660.
[4] A. Agui, S. Shin, M. Fujisawa, Y. Tezuka, T. Ishii, Y. Muramatsu, O. Mishima, K. Era, Phys. Rev. B 55 (1997) 2073.
[5] J.J. Jia, T.A. Callcott, E.L. Shirley, J.A. Carlisle, L.J. Terminello, A. Asfaw, D.L. Ederer, F.J. Himpsel, R.C.C. Perera, Phys. Rev. Lett. 76 (1996) 4054.
[6] J.A. Carlisle, E.L. Shirley, E.A. Hudson, L.J. Terminello, T.A. Callcott, J.J. Jia, D.L. Ederer, R.C.C. Perera, F.J. Himpsel, Phys. Rev. Lett. 74 (1995) 1234.
[7] Y. Ma, N. Wassdahl, P. Skytt, J. Guo, J. Nordgren, P.D. Johnson, J.-E. Rubensson, T. Boske, W. Eberhardt, S.D. Kevan, Phys. Rev. Lett. 69 (1992) 2598.
[8] S.M. Butorin, J.-H. Guo, M. Magnuson, J. Nordgren, Phys. Rev. B 55 (1997) 4242.
[9] F.M.F. de Groot, P. Kuiper, G.A. Sawatzky, Phys. Rev. B 57 (1998) 14584.
[10] L. Braicovich, C. Dallera, G. Ghiringhelli, N.B. Brookes, J.B. Goedkoop, M.A. van Veenendaal, Phys. Rev. B 55 (1997) 15989.
[11] A. Moewes, . Ederer, M.M. Grush, T.A. Callcott, Phys. Rev. B 59 (1999) 5452.
[12] Y. Tezuka, S. Shin, A. Agui, M. Fujisawa, T. Ishii, J. Phys. Soc. Jpn. 65 (1996) 312.
[13] S. Shin, M. Fujisawa, H. Ishii, Y. Harada, M. Watanabe, M.M. Grush, T.A. Callcott, R.C.C. Perera, E.Z. Kurmaev, A. Moewes, R. Winarski, S. Stadler, D.L. Ederer, J. Electron Spectrosc. Relat. Phenom. 92 (1998) 197.
[14] S.M. Butorin, J.-H. Guo, M. Magnuson, P. Kuiper, J. Nordgren, Phys. Rev. B 54 (1996) 4405.
[15] J. Jiménez-Mier, J. van Kd, D.L. Ederer, T.A. Callcott, J.J. Jia, J. Carlisle, L. Terminello, A. Asfaw, R.C. Perera, Phys. Rev. B 59 (1999) 2649.
[16] C.-C. Kao, W.A.L. Caliebe, J.B. Hastings, J.-M. Gillet, Phys. Rev. B 54 (1996) 16361.

[17] S.M. Butorin, D.C. Mancini, J.-H. Guo, N. Wassdahl, J. Nordgren, M. Nakazawa, S. Tanaka, T. Uozumi, A. Kotani, Y. Ma, K.E. Miyano, B.A. Karlin, D.K. Shuh, Phys. Rev. Lett. 77 (1996) 574.
[18] F. Gel'mukhanov, H. Ågren, Phys. Rev. A 49 (1994) 4378.
[19] P. Kuiper, J.-H. Guo, C. Sathe, L.-C. Duda, J. Nordgren, J.J.M. Pothuizen, F.M.F. deGroot, G.A. Sawatzky, Phys. Rev. Lett 80 (1998) 5204.
[20] Y. Harada, H. Ishii, M. Fujisawa, Y. Tezuka, S. Shin, M. Watanabe, Y. Kitajima, A. Yagishita, J. Sync. Rad. 5 (1998) 1013.
[21] H. Ohashi, E. Ishiguro, Y. Tamenori, H. Kishimoto, M. Tanaka, M. Irie, T. Ishikawa, Nucl. Instrum. Methods A 467–468 (2001) 529.
[22] T. Tokushima, Y. Harada, M. Watanabe, Y. Takata, E. Ishiguro, A. Hiraya, S. Shin, Surf. Rev. Lett. 9 (2002) 503.
[23] Y. Harada, T. Kinugasa, R. Eguchi, M. Matsubara, A. Kotani, M. Watanable, A. Yagishita, S. Shin, Phys. Rev. B 61 (2000) 12854.
[24] K. Okada, A. Kotani, J. Electron Spectrosc. Relat. Phenom. 62 (1993) 131.
[25] T. Idé, A. Kotani, J. Phys. Soc. Jpn. 67 (1998) 3621.
[26] S.-D. Mo, W.Y. Ching, Phys. Rev. B 51 (1995) 13023.
[27] B. Poulmellec, P.J. Durham, G.Y. Guo, J. Phys. Condens. Matter 3 (1991) 8195.
[28] N. Daude, C. Gout, L. Journin, Phys. Rev. B 15 (1977) 3229.
[29] K. Vos, J. Phys. C10 (1977) 3917.
[30] L.B. Lin, S.D. Mo, D.L. Lin, J. Phys. Chem. Solids 54 (1993) 907.
[31] A. Hagfeldt, H. Siegbahn, S.-E. Lindquist, S. Lunell, Int. J. Quantum Chem. 44 (1992) 477.
[32] M. Cardona, G. Harbeke, Phys. Rev. 137 (1965) A1467.
[33] S.K. Sen, J. Riga, J. Verbist, Chem. Phys. Lett. 39 (1976) 560.
[34] M.A. Khan, A. Kotani, J.C. Parlebas, J. Phys. Condens. Matter 3 (1991) 1763.
[35] T. Jo, A. Tanaka, J. Phys. Soc. Jpn. 64 (1995) 676.
[36] K.C. Prince, V.R. Dhanak, P. Finetti, J.F. Walsh, R. Davis, C.A. Muryn, H.S. Dhariwal, G. Thornton, G. va der, Phys. Rev. B 55 (1997) 9520.
[37] T. Uozumi, K. Okada, A. Kotani, J. Phys. Soc. Jpn. 62 (1993) 2595.
[38] Y. Tezuka, S. Shin, T. Ishii, T. Ejima, S. Suzuki, S. Sato, J. Phys. Soc. Jpn. 63 (1994) 347.
[39] M. Matsubara, T. Uozumi, A. Kotani, Y. Harada, S. Shin, J. Phys. Soc. Jpn. 71 (2002) 347.
[40] F. Reinert, P. Steiner, R. Zimmermann, R. Claessen, S. Hüfner, Z. Phys. B 99 (1996) 229;
F. Reinert, S. Kumar, P. Steiner, R. Claessen, S. Hüfner, Z. Phys. B 94 (1994) 431.
[41] Y. Harada, K. Okada, R. Eguchi, A. Kotani, H. Takagi, T. Takeuchi, S. Shin, Phys. Rev. B 66 (2002) 165104.
[42] P.W. Anderson, Science 235 (1987) 1196.
[43] F.C. Zhang, T.M. Rice, Phys. Rev. B 37 (1988) 3759.
[44] P. Abbamonte, C.A. Burns, E.D. Isaacs, P.M. Platzman, L.L. Miller, S.W. Cheong, M.V. Klein, Phys. Rev. Lett. 83 (1999) 860.
[45] J.P. Hill, C.-C. Kao, W.A.L. Caliebe, M. Matsubara, A. Kotani, J.L. Peng, R.L. Greene, Phys. Rev. Lett. 80 (1998) 4967.
[46] T. Idé, A. Kotani, J. Phys. Soc. Jpn. 69 (2000) 3107.
[47] K. Okada, A. Kotani, Phys. Rev. B 65 (2002) 144530.
[48] G. Blumberg, P. Abbamonte, M.V. Klein, W.C. Lee, D.M. Ginsberg, L.L. Miller, A. Zibold, Phys. Rev. B 53 (1996) R11930.